Original Article

DOI: 10.5582/irdr.2021.01138

Pan-cancer analysis of osteogenesis imperfecta causing gene *SERPINF1*

Chao Zhang, Wei Yang, Shanshan Zhang, Yongtao Zhang, Pengchao Liu, Xianxian Li, Wei Zhi, Dan Yang, Mian Li, Yanqin Lu*

Key Laboratory for Biotech-Drugs of National Health Commission, Key Laboratory for Rare & Uncommon Diseases of Shandong Province, Biomedical Sciences College & Shandong Medicinal Biotechnology Centre, Shandong First Medical University & Shandong Academy of Medical Sciences, Ji'nan, China.

SUMMARY Osteogenesis imperfecta (OI) type VI causative gene *SERPINF1*, encodes a member of the serpin family that does not display the serine protease inhibitory activity shown by many of the other serpin proteins. The encoded protein (pigment epithelium-derived factor, PEDF) has anti-tumor, anti-angiogenesis, anti-inflammation, nutrition and nerve protection functions, and participates in fat metabolism. In this paper, a series of bioinformatics analyses were conducted based on the regulation of *SERPINF1* in the human. Pan-cancer analysis of *SERPINF1* revealed it to play a role in the prognosis of tumors, especially in KIRC, and that high expression of *SERPINF1* leads to a poor prognosis of the disease, the occurrence of which is largely related to the high expression of *SERPINF1* leading to immune infiltration of cancer associated fibroblasts. Mutation analysis found that *SERPINF1* had eight identical amino acids alterations sites with different in both cancer and OI patients. which hints the possible relationship between genotype and phenotype.

Keywords *SERPINF1*, osteogenesis imperfecta, pan-cancer analysis, cancer

1. Introduction

Osteogenesis imperfecta (OI) type VI disease-causing gene, *SERPINF1*, located on chromosome 17P13.3 encodes for pigment epithelium-derived factor (PEDF), which is expressed actively in adult bone, especially in active bone growth sites (*1,2*). PEDF belongs to the serpin super family, functions in anti-tumor, anti-angiogenesis, anti-inflammation, nutrition and nerve protection, and participates in fat metabolism (*3-6*).

In bone, PEDF can promote the differentiation and mineralization of osteoblasts, facilitate the gene expression of osteoblasts, inhibit the maturation of osteoclasts, and activate the Wnt/β-Catenin signal transduction pathway (*2,7,8*). In osteoblasts, PEDF can hardly be detected in the serum of patients with osteogenesis imperfecta induced by *SERPINF1* mutation (*9*). In tumors, PEDF selectively induces apoptosis of endothelial cells in vessels undergoing remodeling (*4*). PEDF has also been shown to have suppressor-like activity *in vivo* and directly inhibits tumor growth and metastasis, and reduced PEDF levels have also been associated with a worse prognosis in a variety of tumors (*4*).

In this paper, we used the GCBI website to find the related diseases reported by the *SERPINF1* gene in the article. Through the pan-cancer analysis of *SERPINF1* gene, the potential molecular mechanisms of *SERPINF1* in the pathogenesis or clinical prognosis were found in different cancers. We also analyzed the mutation sites of *SERPINF1* in cancer and osteogenesis imperfecta, to find out the potential diseases connection among these diseases.

2. Methods and Materials

2.1. Gene's research status and regulation mechanism

We input *SERPINF1* in the "Gene radar" module of GCBI (Gene Cloud of Biotechnology Information) web (*https://www.gcbi.com.cn*) and found the research status, regulation network and transcription factor prediction for the *SERPINF1* gene.

2.2. Gene expression analysis

The Human Protein Atlas website (*https://www.proteinatlas.org*) was used to get the expression of *SERPINF1* in different human tissues and cell types (*10,11*).

We used the TIMER2 (tumor immune estimation resource, version 2) website (*http://timer.cistrome.org*) to observe the difference in *SERPINF1* expression between tumor and paracancerous tissues (*12*).

For tumors without normal tissue or highly restricted normal tissue [*e.g.*, TCGA-ACC (The Cancer Genome Atlas, Adrenocortical carcinoma), TCGA-BLCA (Bladder urothelial carcinoma), *etc.*], GEPIA2 (Gene Expression Profiling Interactive Analysis, version 2) was used to obtain the block diagram of the expression difference between these tumor tissues and corresponding normal tissues in the GTEX (genotype tissue expression) database, under the settings of *p*-value cutoff = 0.01, $\log_2$FC (folding change) cutoff = 1 and "matching TCGA normal and GTEX data" (*13*). In addition, we obtained the violin diagram of *SERPINF1* expression in different pathological stages of all TCGA tumors through the "pathological stage diagram" module of GEPIA2 (*13*). The log2 [TPM (Transcripts per million) +1] transformed expression data were applied for the box or violin plots (*13*).

2.3. Survival prognosis analysis

We used the "survival map" in the "survival analysis" module of the GEPIA2 website to obtain the OS (overall survival) and DFS (disease-free survival) map data related to *SERPINF1* in all tumors in TCGA (log rank test as hypothesis test). Cutoff-high (50%) and cutoff-low (50%) values was used as expression thresholds to separate high expression and low expression cohorts in survival maps and survival plots (*13*).

2.4. Immune infiltration analysis

We used the "Immune-Gene" module of the TIMER2 web server to explore the association between *SERPINF1* expression and immune infiltration across all TCGA tumors. CD^{8+} T-cells, CD^{4+} T-cells, neutrophils, cancer-associated fibroblasts and endothelial cells were selected and the TIMER, CIBERSORT, CIBERSORT-ABS, QUANTISEQ, XCELL, MCPCOUNTER and EPIC algorithms were applied for immune infiltration estimations. The *P*-values and partial correlation values were obtained *via* the purity-adjusted Spearman's rank correlation test and the data were visualized as a heatmap and a scatter plot (*12*).

2.5. Genetic alteration analysis

CBioPortal website (*https://www.cbioportal.org*) was used to obtain the change frequency, mutation type and CNA (copy number alteration) of *SERPINF1* gene in all TCGA tumors (*14*). We used the OI website (*https://oi.gene.le.ac.uk*) to find the *SERPINF1* mutations that cause osteogenesis imperfecta (*15*).

2.6. *SERPINF1* -related gene enrichment analysis

The experimentally determined PEDF binding proteins were obtained by us using the string (*https://string-db.org*) website, with the following settings: full network, evidence, experiments, low confidence (0.150), no more than 50 interactors in the first outer shell.

GeneMANIA websites (*http://genemania.org*) helped us find possible interacting genes by searching many large and open biological data sets (*16*).

Venn plot was drawn using (*http://bioinformatics.psb.ugent.be/webtools/Venn*) to conduct an intersection analysis to compare PEDF binding protein and interacting gene. In addition, we performed KEGG pathway analysis and go analysis on these two groups of data. First, the data of function annotation diagram was obtained by using the DAVID website (*https://david.ncifcrf.gov*), and the data with $P < 0.05$ was selected; the enriched paths are displayed by using "tidyr" and "ggplot2" R packages. R package "cluster profiler" was used for GO (gene ontology) enrichment analysis. By using the cnetplot function (circular = F, color edge = T, node tag = T), the data of GO analysis can be visualized as cnetplot. R language software [R-4.0.5, 64-bit] (*https://www.r-project.org*) was used in this analysis.

3. Results

PEDF belongs to serpin superfamily and is actively expressed in adult bone. It has been identified as an OI type VI pathogenic gene (*1,2*). In addition, it has anti-angiogenesis anti-tumor and other functions (*3,4*). In this study, we aimed to provide a comprehensive analysis on the association of human *SERPINF1* (NM_ 001329903.2 for mRNA, NP_ 001316832.1 for protein, Figure S1 A, *http://www.irdrjournal.com/action/getSupplementalData.php?ID=88*) with the development of cancer and the connection between cancer and osteogenesis imperfecta. As shown in Figure S1 B, in different species (*e.g.*, Homo sapiens, Mus musculus, Equus caballus), the structure of PEDF is usually composed of serpin (cl38926) domain. Phylogenetic tree data confirmed that the structure of PEDF is highly conserved across the different species, suggesting that PEDF may play an important role in basic biological processes (Figure S2, *http://www.irdrjournal.com/action/getSupplementalData.php?ID=88*).

3.1. Gene's research status and regulation mechanism

By searching the GCBI database, we found literature reports about *SERPINF1* related to 20 human diseases, and the most reported disease is cancer. OI disease related document number ranked 12th (Figure 1A).

The regulatory network of *SERPINF1* contains one targeted miRNA (hsa-miR-335-5p), 97 related lncRNA, a downstream phosphorylation gene (*EPM2AIP1*) and

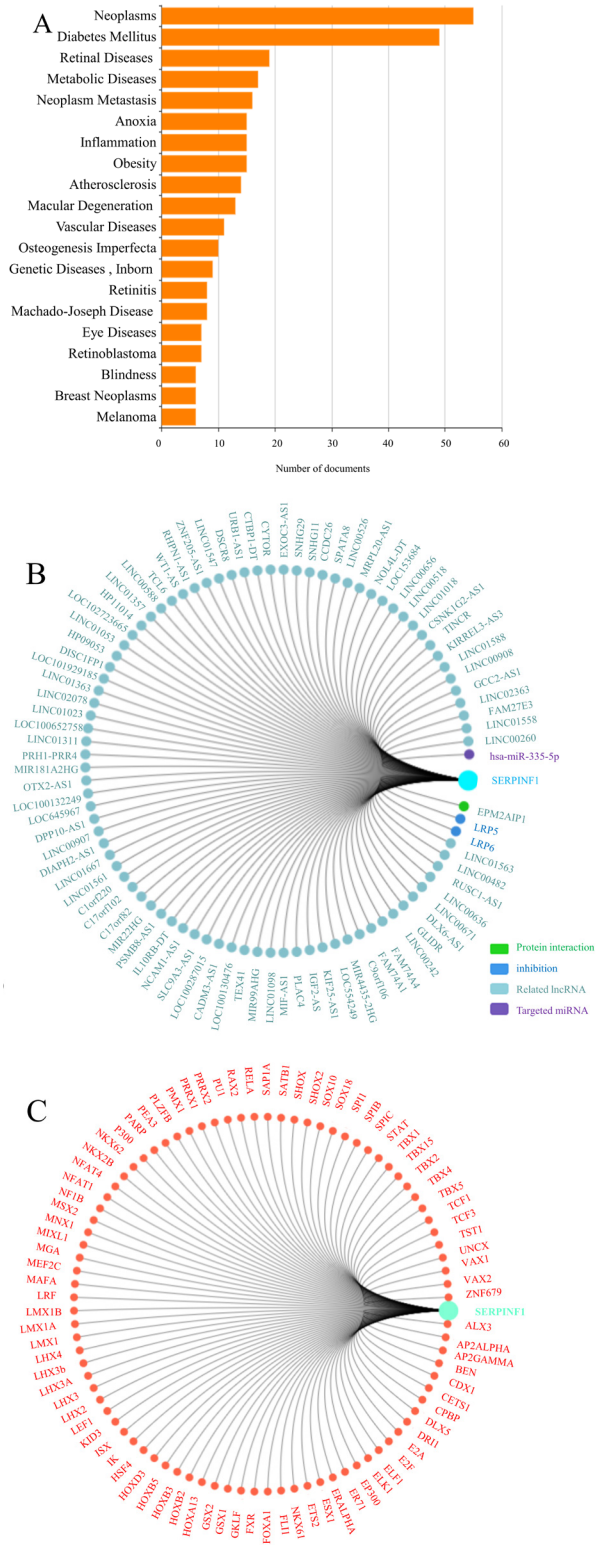

Figure 1. *SERPINF1* research status and regulation mechanism. **(A)** Literature reported about *SERPINF1* in human diseases. **(B)** The regulatory network of *SERPINF1*. **(C)** Transcription factors highly related to *SERPINF1*.

two genes (*LRP5* and *LRP6*) that inhibit *SERPINF1* expression (Figure 1B). Also, there are 87 transcription factors highly associated with *SERPINF1*, which are closely related to the specific expression of *SERPINF1* (Figure 1C)

3.2. Gene expression analysis

We analyzed the expression of *SERPINF1* in different tissues. As shown in Figure S3 (*http://www.irdrjournal.com/action/getSupplementalData.php?ID=88*), *SERPINF1* can be expressed in all detected tissues (all consensus normalized expression values > 0.1). And based on the combination of the HPA (Human protein atlas), GTEx and FANTOM5 (Function annotation of the mammalian genome 5) datasets, *SERPINF1* shows highest expression in the retina, followed by the liver, dendritic cells, and pons and medulla.

We used the TIMER2 website to analyze the expression of *SERPINF1* in different tumor types in the TCGA database. As shown in Figure 2B, the expression level of *SERPINF1* in tumor tissue of BLCA (Bladder Urothelial Carcinoma), BRCA (Breast invasive carcinoma), CHOL (Cholangiocarcinoma), COAD (Colon adenocarcinoma), KICH (Kidney Chromophobe), KIRC (Kidney renal clear cell carcinoma), LUAD (Lung adenocarcinoma), PRAD (Prostate adenocarcinoma), THCA (Thyroid carcinoma), UCEC (Uterine Corpus Endometrial Carcinoma) ($P < 0.001$), CESC (Cervical squamous cell carcinoma and endocervical adenocarcinoma) ($P < 0.01$), GBM (Glioblastoma multiforme), PCPG (Pheochromocytoma and Paraganglioma), and READ (Rectum adenocarcinoma) ($P < 0.05$) is lower than the corresponding control tissues. And the expression of *SERPINF1* in KIRC and LUAD ($P < 0.0001$) is higher than in normal control tissues (Figure 2A).

In cases where tumor and normal tissue data were not available from TCGA, we further evaluated the expression differences of *SERPINF1* between tumor and normal tissues using the GTEX dataset. We found that the expression level of *SERPINF1* in tumor tissue of ACC (Adrenocortical carcinoma), BLCA, BRCA, CESC, CHOL, COAD, KICH, LAML (Acute Myeloid Leukemia), LGG (Brain Lower Grade Glioma), OV (Ovarian serous cystadenocarcinoma), PRAD, READ, TGCT (Testicular Germ Cell Tumors), THCA, UCEC and UCS (Uterine Carcinosarcoma) ($P < 0.01$) is lower than the corresponding control tissues (Figure 2B). And the expression of *SERPINF1* in DLBC (Lymphoid Neoplasm Diffuse Large B-cell Lymphoma), KIRC, PRAD and THYM (Thymoma) ($P < 0.01$) is higher than in normal control tissues (Figure 2C). There was no significant difference in *SERPINF1* expression in other cancers [*e.g.*, LUAD, ESCA (Esophageal carcinoma), GBM, HNSC (Head and Neck squamous cell carcinoma), and KIRP (Kidney renal papillary cell carcinoma)], as shown in Figure S4 (*http://www.irdrjournal.com/action/getSupplementalData.php?ID=88*).

GEPIA2 was used to obtain the expression map of *SERPINF1* at different stages of tumors (Figure S5, *http://www.irdrjournal.com/action/getSupplementalData.php?ID=88*). Among them, the

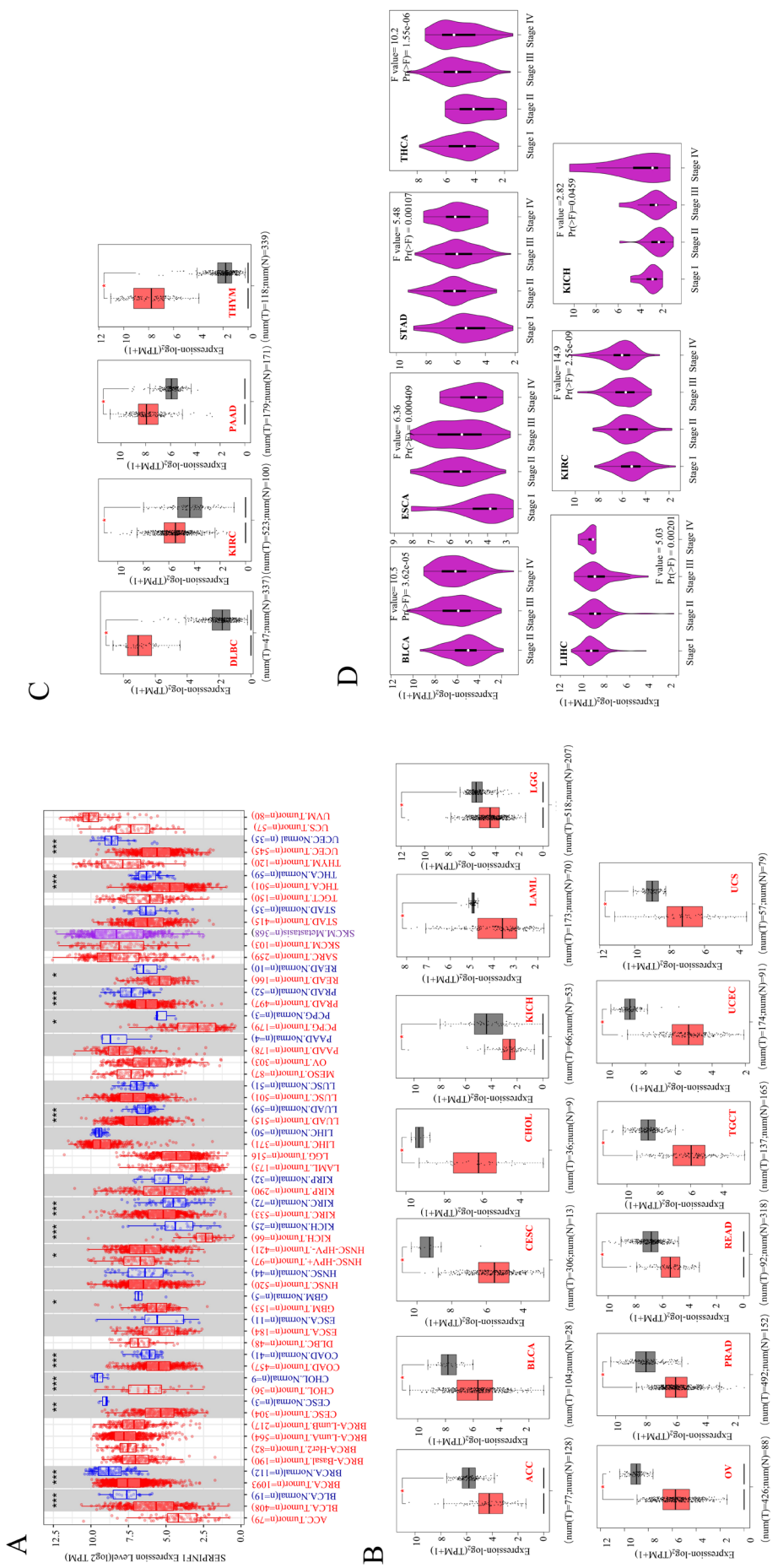

Figure 2. *SERPINF1* expression analysis data. (A) Expression levels of *SERPINF1* in TCGA tumor *vs.* adjacent tissues as visualized by TIMER2. $^{*}P < 0.05$; $^{**}P < 0.01$; $^{***}P < 0.001$. **(B)** *SERPINF1* high expression in tumor tissues by using GEPIA2 website to analyze the expression of *SERPINF1* in different types of cancer (for tumor with no normal tissue or highly restricted normal tissue in TCGA) matched with TCGA normal and GTEx data. **(C)** *SERPINF1* low expression in cancer tissues by using GEPIA2 website to analyze the expression of *SERPINF1* in different types of cancer (for tumor with no normal tissue or highly restricted normal tissue in TCGA) matched with TCGA normal and GTEx data. **(D)** Stage-dependent expression level of *SERPINF1*.

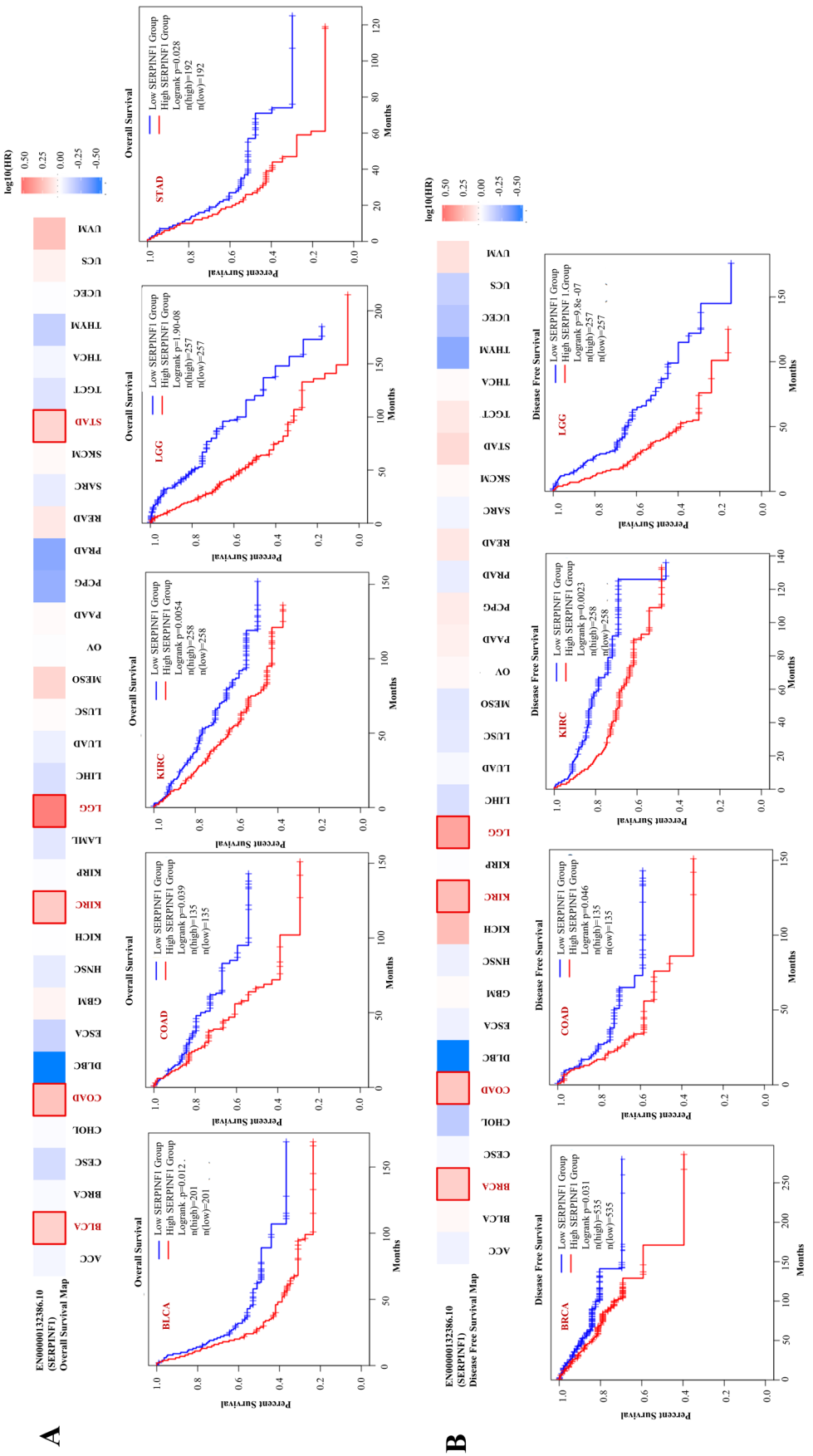

Figure 3. Relationship between *SERPINF1* expression and survival rate in TCGA tumors. **(A)** Relationship between *SERPINF1* gene expression and survival (overall survival). **(B)** Relationship between *SERPINF1* gene expression and survival (disease-free survival).

expression of *SERPINF1* was variable at different stages of ACC, BLCA, CESC, COAD, KICH, LUAD, PAAD, and THCA (Figure 2E, all $P < 0.05$) (Figure 2D).

3.3. Survival analysis data

TCGA and GEO data sets were used to study the correlation between *SERPINF1* expression and prognosis of different tumor patients. As shown in Figure 3A, high expression of *SERPINF1* was associated with poor OS (overall survival) prognosis of BLCA (P = 0.012), COAD (P = 0.039), KIRC (P = 0.0054), LGG (P = 1.9e-8) and STAD (P = 0.028) in TCGA program. Disease-free survival (DFS) analysis data disclosed that a correlation between high *SERPINF1* expression and poor prognosis in TCGA cases of BRCA (P = 9.8e-07), COAD (P = 0.0023), KIRC (P = 0.046) and LGG (P = 0.031) (Figure 3B). It is noteworthy that the high expression of *SERPINF1* leads to a decrease in the OS and DFS survival curves of COAD, KIRC and LGG.

3.4. Immune infiltration analysis data

As an important component of the tumor microenvironment, tumor infiltrating immune cells are closely associated with cancer initiation, progression or metastasis (*17,18*). Cancer associated fibroblasts in tumor microenvironments have been reported to be involved in regulating the function of various tumor infiltrating immune cells and play a key role in tumor adaptation to the host (*19-21*). Here, we used the XCELL, MCPCOUNTER, EPIC and TIDE algorithms to investigate the potential relationship between the level of infiltration of cancer associated fibroblasts and *SERPINF1* gene expression in different TCGA cancer types.

As shown in Figure 4, *SERPINF1* expression in the vast majority of tumors was statistically positively correlated with the value of cancer associated fibroblast infiltration and endothelial cells, but the infiltration ability of CD^{4+} T cells, CD^{8+} T cells, and neutrophils did not correlate with the expression of *SERPINF1*.

It is noteworthy that in KIRC and THCA, the infiltrative capacity of endothelial cells inversely correlated with the expression of *SERPINF1*.

3.5. Genetic alteration analysis data

We observed the genetic alteration status of *SERPINF1* in different tumor samples of the TCGA cohort. As shown in Figure 5A, the highest alteration frequency (> 4%) of *SERPINF1* was present in patients with uterine tumors of the predominant type with "mutations". It is worth noting that the "deep deletion" type of CNA is the predominant type in diffuse large B-cell lymphoma, thymoma, thyroid cancer, acute myeloid leukemia, and pancreatic cancer, whereas "amplified" type CNA are the predominant mutation type in uterine carcinosarcoma, renal clear cell carcinoma, and brain lower grade glioma. The type, location, and number of cases with alterations of *SERPINF1* are further shown in Figure 5A. We found that missense mutations in *SERPINF1* were the predominant type of genetic alteration, with 58 missense mutations, 11 truncating mutations, and one in-frame mutation, with the largest number of duplications (4 times) at the X147_splice/K147K and R99Q loci (Figure 5B, Table S1, *http://www.irdrjournal.com/action/getSupplementalData.php?ID=88*).

From OI database, we found 45 *SERPINF1* mutations reported (Table S2, *http://www.irdrjournal.com/action/getSupplementalData.php?ID=88*) (*15,22*). No common mutation sites were found by comparing the mutation sites of *SERPINF1* in tumors and OI patients. Then, we analyzed whether there were changes in the same amino acids in tumor and OI patients and found eight identical site amino acid with different changes. They are sites 27, 56, 99, 131, 133, 147, 178, and 201, which may lead to different functions of the PEDF and has been associated with tumor prognosis and osteogenesis (Table 1). Significantly, alterations of the amino acids at positions 99 and 147 of *SERPINF1* were the most recurrent in tumors (4 times).

3.6. *SERPINF1*-related gene enrichment analysis date

To further investigate the molecular mechanism of *SERPINF1*, we attempted to screen *SERPINF1* binding proteins and *SERPINF1* expression related genes for a series of pathway enrichment analyses. Based on the string tool, we obtained a total of 31 *SERPINF1* binding proteins that are supported by experimental evidence. The interaction network of these proteins is shown in Figure 6A.

GeneMANIA predicts 20 genes related to *SERPINF1* co-expression, as shown in Figure 6B. GeneMANIA and String web together predicted 48 genes related to the function of *SERPINF1*. Venn plot shows that they have three common members, namely, *EPM2AIP1*, *PNPLA2* and *SERPINA6* (Figure 6C).

We combined the String and GeneMANIA two datasets to perform KEGG and GO enrichment analyses. The KEGG data suggest that "Viral carcinogenesis", "PI3K-Akt signaling pathway" and "cell cycle" might be involved in the effect of *SERPINF1* functions ((Figure 6D). GO enrichment analysis data further show that most of these genes are related to protein metabolism pathways or components and functions of extracellular mechanisms, *e.g.*, extracellular matrix structural constituent, cadherin binding, collagen-containing extracellular matrix, complex of collagen trimers and others. (Figure 6, E-G).

4. Discussion

SERPINF1 is a causative gene for osteogenesis imperfecta, and by searching the GCBI database, we

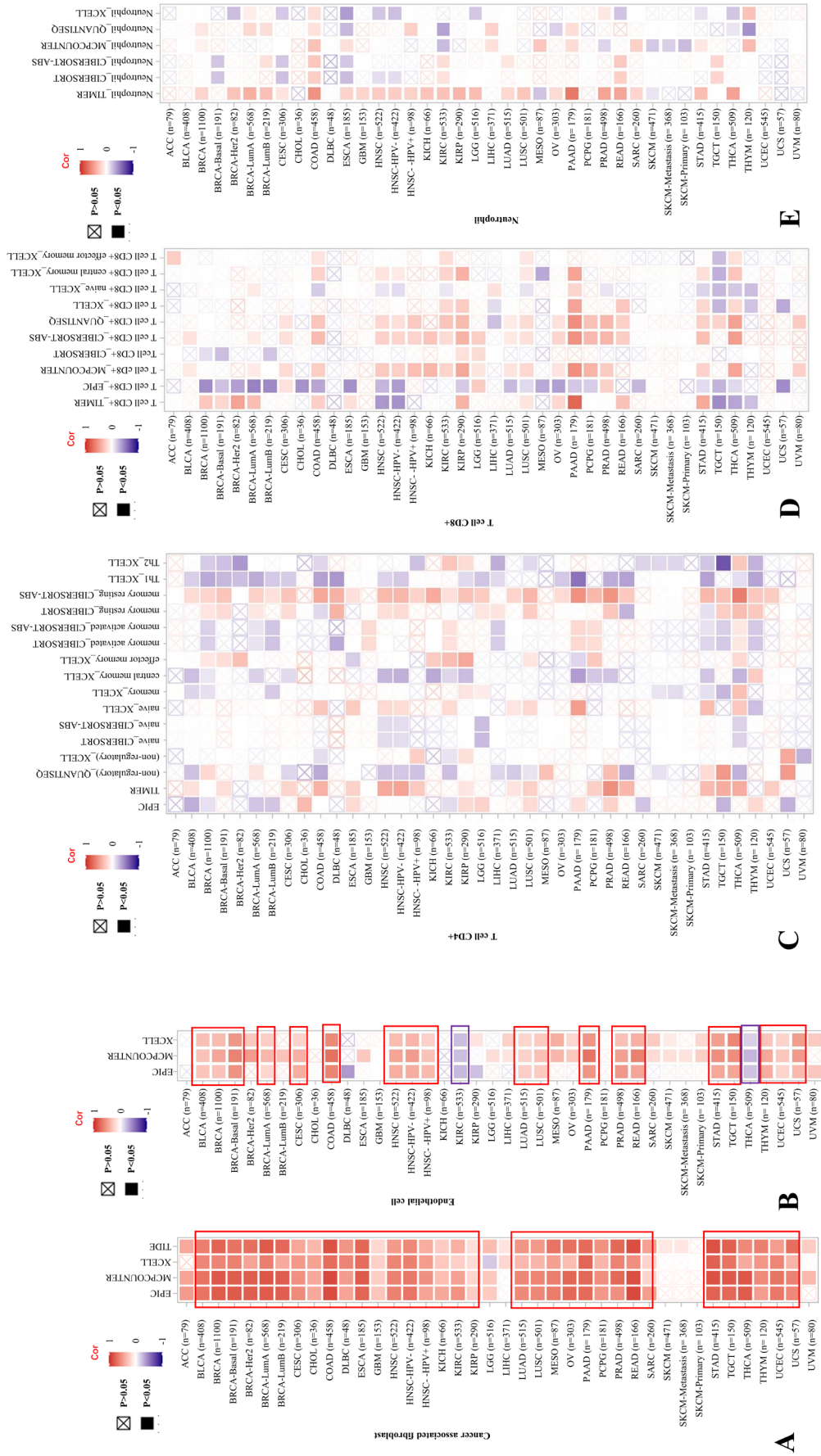

Figure 4. The correlation between *SERPINF1* expression level and infiltration of cancer-associated fibroblasts, endothelial cells, CD^{8+} T cells, CD^{4+} T cells, and neutrophils. (A-E) TIMER, CIBERSORT, CIBERSORT-ABS, TIDE, XCELL, MCPCOUNTER, QUANTISEQ and EPIC algorithms were used for the correlative analysis of the level of cancer-associated fibroblasts, endothelial cells, CD8+ T cells, CD4+ T cells, and neutrophils and the expression levels of the *SERPINF1* gene across all tumors in TCGA. The red color indicates a positive correlation (0–1), while the blue color represents a negative correlation (−1–0). The correlation with *P*-value < 0.05 is considered statistically significant. Statistically insignificant correlation values are marked with crosses.

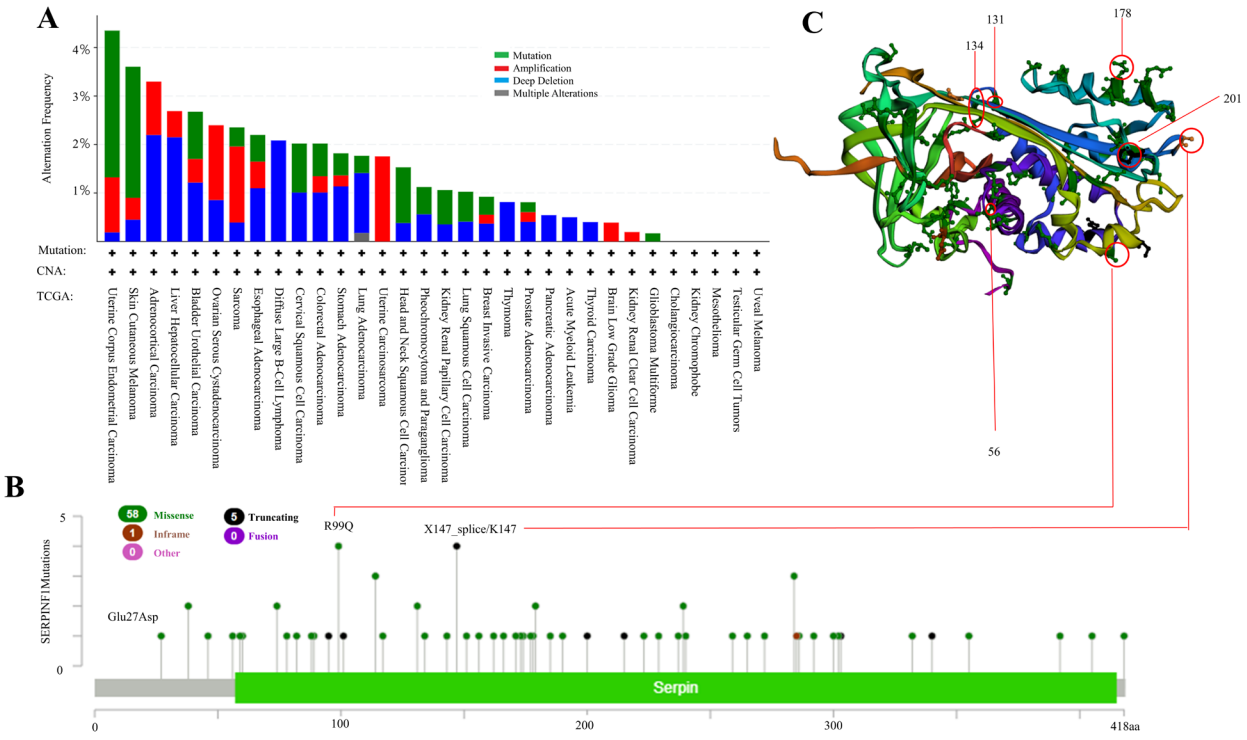

Figure 5. Mutation status of *SERPINF1* in TCGA tumors. (A) The alteration frequency with mutation type. **(B)** Mutation site. **(C)** Mutation site (56, 99, 131, 147, 178, 201) are shown in the 3D structure of *SERPINF1*.

Table 1. PEDF Change at the same sites in Cancer and OI

Cancer	OI
Glu27Asp	Glu27Glyfs*38
Ala56Val	Ala56Gly
Arg99Gln	Arg99*
Ala131Val	Ala131Asp
Gln133Argfs*18	Gln133*
X147_splice	Lys147_Gly215delArg
Gln178His	Gln178*
Asp201Metfs*18	Asp201Asn

found that there are literature reports that *SERPINF1* is associated with 20 human diseases, and the most frequently reported disease is cancer. In our study, homologous genes and phylogenetic tree data confirm the conservatism of PEDF structure in different species, but additional functional gain and functional loss studies are needed to further explore its functions in different cellular environments.

An increasing number of studies focus on the function of *SERPINF1* in diseases including cancer. It remains to be answered whether *SERPINF1* can play a role in the pathogenesis of different tumors through some common molecular mechanisms. Through literature search, we have not retrieved any publications from the overall cancer perspective for *SERPINF1* pan-cancer analysis. Therefore, based on the data of TCGA, CPTAC and GEO database, gene expression and gene change, we detected the *SERPINF1* gene in 33 different tumors. In addition, we compared the mutation sites of cancer with those of osteogenesis imperfecta, and found that there were 8 amino acids at the same sites, at positions 27, 56, 99, 131, 133, 147, 178, and 201. Mutations in the *SERPINF1* gene lead to the development of osteogenesis imperfecta, but whether these mutations are linked to tumorigenesis will require more data and studies to prove.

The results showed that the expression level of *SERPINF1* in tumor tissues of ACC, BLCA, BRCA, CESC, CESC, CHOL, COAD, GBM, KICH, KICH, KIRC, LAML, LGG, LUAD, OV, PCPG, PRAD, READ, TGCT, THCA, UCEC, UCS was lower than that of the corresponding control group, whereas higher expression was observed in DLBC, KIRC, PRAD and THYM.

Differences in *SERPINF1* expression levels in different tumor types may reflect different underlying functions and mechanisms. We further found that for patients with tumors with high expression of *SERPINF1*, such as BLCA, COAD, KIRC, LGG and STAD, overexpression of *SERPINF1* generally predicted poor OS. It is noteworthy that the high expression of *SERPINF1* leads to a decrease in the OS and DFS curves of COAD, KIRC and LGG. These results suggest that *SERPINF1* is a potential biomarker for predicting the prognosis of patients with tumors. Especially in KIRC, we found that *SERPINF1* expression was higher than in the control group ($P < 0.01$), and the high expression of *SERPINF1* was associated with poor prognosis of OS ($P = 0.0054$) and DFS ($P = 0.0023$).

SERPINF1 has been reported to have antitumor

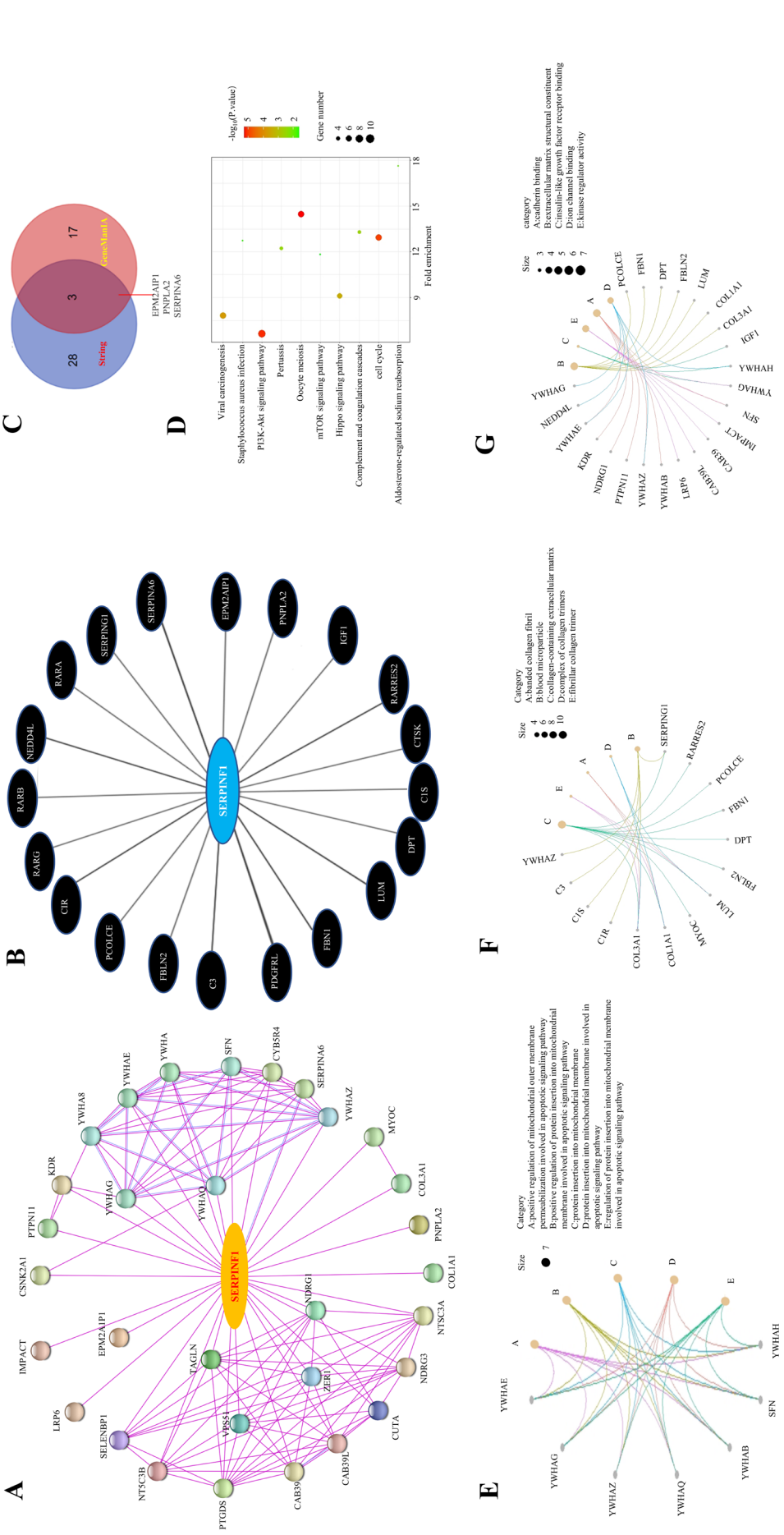

Figure 6. *SERPINF1*-related gene enrichment and pathway analysis. (A) STRING protein network map of experimentally determined PEDF-binding proteins. **(B)** GeneMANIA predicted gene network diagram associated with *SERPINF1* co-expression. **(C)** Venn plot of (A) and (B). **(D)** KEGG pathway analysis based on the *SERPINF1*-binding and co-expression genes. **(E)** GO pathway analysis (Biological Process, BP) based on the *SERPINF1*-binding and co-expression genes. **(F)** GO pathway analysis (Cellular Component, CC) based on the *SERPINF1*-binding and co-expression genes. **(G)** GO pathway analysis (Molecular Function, MF) based on the *SERPINF1*-binding and co-expression genes.

effects (*4*). It is doubtful that high expression of *SERPINF1* leads to poor prognosis in cancer, such as COAD, LGG and KIRC. It has been reported that the tumor microenvironment is related to the occurrence and development of cancer (*18*). Our immune infiltration analysis showed that the high expression of *SERPINF1* was not related to infiltration of immune cells, but positively correlated with the infiltration ability of cancer associated fibroblasts and endothelial cells. Interestingly, in KIRC, high *SERPINF1* expression was inversely correlated with the invasive capacity of endothelial cells, indicating that infiltration of cancer associated fibroblasts is an important factor leading to poor prognosis of KIRC.

In conclusion, from our bioinformatics analysis of *SERPINF1*, we found that there were 8 amino acid changes at the same locus in OI and cancer. But more data and studies are needed to determine their relation to the occurrence of cancer. From our comprehensive pan-cancer analysis of *SERPINF1*, it is helpful to elucidate the role of *SERPINF1* in tumor development from multiple perspectives.

Funding: This work was supported by a grant from the Shandong government (2018WS178) and the Academic Promotion Programme of Shandong First Medical University (LJ001).

Conflict of Interest: The authors have no conflicts of interest to disclose.

References

1. Broadhead ML, Akiyama T, Choong PF, Dass CR. The pathophysiological role of PEDF in bone diseases. Curr Mol Med. 2010; 10:296-301.
2. Becker J, Semler O, Gilissen C, *et al.* Exome sequencing identifies truncating mutations in human *SERPINF1* in autosomal-recessive osteogenesis imperfecta. Am J Hum Genet. 2011; 88:362-371.
3. Mejias M, Coch L, Berzigotti A, Garcia-Pras E, Gallego J, Bosch J, Fernandez M. Antiangiogenic and antifibrogenic activity of pigment epithelium-derived factor (PEDF) in bile duct-ligated portal hypertensive rats. Gut. 2015; 64:657-666.
4. Becerra SP, Notario V. The effects of PEDF on cancer biology: mechanisms of action and therapeutic potential. Nat Rev Cancer. 2013; 13:258-271.
5. Sanchez A, Tripathy D, Yin X, Luo J, Martinez J, Grammas P. Pigment epithelium-derived factor (PEDF) protects cortical neurons *in vitro* from oxidant injury by activation of extracellular signal-regulated kinase (ERK) 1/2 and induction of Bcl-2. Neurosci Res. 2012; 72:1-8.
6. Borg ML, Andrews ZB, Duh EJ, Zechner R, Meikle PJ, Watt MJ. Pigment epithelium-derived factor regulates lipid metabolism *via* adipose triglyceride lipase. Diabetes. 2011; 60:1458-1466.
7. Farber CR, Reich A, Barnes AM, Becerra P, Rauch F, Cabral WA, Bae A, Quinlan A, Glorieux FH, Clemens TL, Marini JC. A novel IFITM5 mutation in severe atypical osteogenesis imperfecta type VI impairs osteoblast production of pigment epithelium-derived factor. J Bone Miner Res. 2014; 29:1402-1411.
8. Glorieux FH, Ward LM, Rauch F, Lalic L, Roughley PJ, Travers R. Osteogenesis imperfecta type VI: a form of brittle bone disease with a mineralization defect. J Bone Miner Res. 2002; 17:30-38.
9. Wang JY, Liu Y, Song LJ, Lv F, Xu XJ, San A, Wang J, Yang HM, Yang ZY, Jiang Y, Wang O, Xia WB, Xing XP, Li M. Novel Mutations in *SERPINF1* Result in Rare Osteogenesis Imperfecta Type VI. Calcif Tissue Int. 2017; 100:55-66.
10. Uhlén M, Fagerberg L, Hallström BM, *et al.* Proteomics. Tissue-based map of the human proteome. Science. 2015; 347:1260419.
11. Thul PJ, Åkesson L, Wiking M, *et al.* A subcellular map of the human proteome. Science. 2017; 356.
12. Li T, Fu J, Zeng Z, Cohen D, Li J, Chen Q, Li B, Liu XS. TIMER2.0 for analysis of tumor-infiltrating immune cells. Nucleic Acids Res. 2020; 48:W509-W514.
13. Tang Z, Li C, Kang B, Gao G, Li C, Zhang Z. GEPIA: a web server for cancer and normal gene expression profiling and interactive analyses. Nucleic Acids Res. 2017; 45:W98-W102.
14. Cerami E, Gao J, Dogrusoz U, *et al.* The cBio cancer genomics portal: an open platform for exploring multidimensional cancer genomics data. Cancer Discov. 2012; 2:401-404.
15. Dalgleish R. The human type I collagen mutation database. Nucleic Acids Res. 1997; 25:181-187.
16. Warde-Farley D, Donaldson SL, Comes O, *et al.* The GeneMANIA prediction server: biological network integration for gene prioritization and predicting gene function. Nucleic Acids Res. 2010; 38:W214-W220.
17. Steven A, Seliger B. The role of immune escape and immune cell infiltration in breast cancer. Breast Care (Basel). 2018; 13:16-21.
18. Fridman WH, Galon J, Dieu-Nosjean MC, Cremer I, Fisson S, Damotte D, Pagès F, Tartour E, Sautès-Fridman C. Immune infiltration in human cancer: prognostic significance and disease control. Curr Top Microbiol Immunol. 2011; 344:1-24.
19. Chen X, Song E. Turning foes to friends: targeting cancer-associated fibroblasts. Nat Rev Drug Discov. 2019; 18:99-115.
20. Kwa MQ, Herum KM, Brakebusch C. Cancer-associated fibroblasts: how do they contribute to metastasis? Clin Exp Metastasis. 2019; 36:71-86.
21. Fearon DT. The carcinoma-associated fibroblast expressing fibroblast activation protein and escape from immune surveillance. Cancer Immunol Res. 2014; 2:187-193.
22. Dalgleish R. The human collagen mutation database 1998. Nucleic Acids Res. 1998; 26:253-255.

Received September 2, 2021; Revised January 23, 2022; Accepted January 31, 2022.

**Address correspondence to:*
Yanqin Lu, Shandong First Medical University & Shandong Academy of Medical Sciences, #6699 Qingdao Road, Ji'nan 250117, China.
E-mail: yqlu@sdfmu.edu.cn (YL)

Released online in J-STAGE as advance publication February 7, 2022.